The *aceE* involves in mycolic acid synthesis and biofilm formation in *Mycobacterium smegmatis*

Suting Chen, Tianlu Teng, Shuan Wen, Tingting Zhang, Hairong Huang*

National Clinical Laboratory on Tuberculosis, Beijing Key laboratory for Drug Resistant Tuberculosis Research, Beijing Chest Hospital, Capital Medical University, Beijing Tuberculosis and Thoracic Tumor Institute, Beijing, China 101149

* Correspondence: huanghairong@tb123.org

Running title: *aceE* involves in cell wall formation of mycobacteria

Abstract

Background: The integrity of cell wall structure is highly significant for the *in vivo* survival for mycobacteria. However, the mechanisms underlying the biosynthesis of mycobacterial cell wall remain poorly understood. *aceE* encodes the E1 component of pyruvate dehydrogenase (PDH) complex. This study aimed to know the functional role of *aceE* gene in cell wall biosynthesis in *M. smegmatis*.

Results: We observed that the colony morphology of *aceE*-deficient mutants (*aceE*-mut) was quite different from the wild-type (WT) strain during the transposon library screening of *M. smegmatis*, smaller and smoother on the solid culture medium. Notably, the *aceE*-mut lost its ability of growing aggregately and biofilm forming, which are two very important features of mycobacteria. The morphological changes of the *aceE*-mut strain were further confirmed by electron microscopy that presented shorter, smoother and thinner images in contrast with WT strain. Additionally, the analysis of mycolic acid (MA) using LC-MS indicated deficiency of alpha-MA and epoxy-MA in *aceE*-mut strain whereas complementation of the *aceE*-mut with a wild-type *aceE* gene restored the composition of MA.

Conclusions: Over all, this study indicates that *aceE* gene plays a significant role in the mycolic acid synthesis and affects the colony morphology and biofilm formation of *M. smegmatis*.

Keywords: *mycobacterium smegmatis*; *aceE*; biofilm; mycolic acid; cell wall

Background

In 1940s, the spread of *Mycobacterium tuberculosis* (Mtb) was controlled to some extent by the discovery of anti-tuberculosis (anti-TB) drugs. However, TB caused by Mtb, still remains one of the most deadly infectious diseases [1, 2]. In both latent and active TB infections, majority of the mycobacteria maintain an extremely low growth rate and survive for longer periods in the phagosome of hosts' macrophages [3, 4].Studies targeting the metabolic pathways that sustain the survival and continual infection of Mtb *in vivo* [4-6] have identified cell wall synthase and its regulatory factors as possible targets for new anti-TB drug development.

The cell wall of mycobacterium genus is mainly composed of three types of macromolecules i.e. peptidoglycan, arabino-galactan and mycolic acids (specific components of mycobacterium genus). The carboxyl of mycolic acids is vertically covalently linked to the hydroxyl group of arabino-galactan by ester bond, arabino-galactan is linked to the peptidoglycan layer by phospholipid bond, whereas other glycolipids and free lipids are regularly distributed in mycolic acids [7]. These collectively form a thick, dense, poorly permeable cell wall, which not only allows mycobacteria to resist the drying environment and harmful chemicals but also allows it to reproduce in the macrophages [8, 9]. Therefore, the molecules involved in the cell wall biosynthesis of TB bacilli have been considered as important anti-TB drug targets. Among the existing anti-TB drugs, isoniazid, ethylamine and ethambutol target the cell wall synthesis pathways, among which isoniazid and ethambutol are the first-line anti-TB drugs.

Pyruvate dehydrogenase (PDH) is an enzyme complex that catalyzes the conversion of pyruvate into acetyl-coA *in vivo*. The complex mainly consists of three enzymes, which are respectively called E1, E2 and E3 components of PDH according to the order in which they participate in the reactions. Through a series of chemical reactions of pyruvate decarboxylation, the glycolytic pathway (the final product is pyruvate) and the tricarboxylic acid cycle (the initial reactant is acetyl-coA) can be effectively connected [10]. As an important intermediate metabolite,

acetyl-coA not only participates in tricarboxylic acid cycle as well as the glyoxylate cycle but also provides carbon source for the synthesis of mycolic acid and lipids. Studies have also found that the genes involved in gluconeogenic pathway and glyoxylate cycle are up-regulated in Mtb isolated from macrophages, mouse lung tissues and tissue samples of patients, suggesting that the compensatory metabolism of acetyl-coA is necessary for intracellular growth and persistence *in vivo* [11, 12].

In the present study, we found a mutant strain of which the *aceE* gene, encoding the E1 component of PDH, was inactivated by Himar1 transposon insertion (*aceE*-mut). This mutant had obvious differences in colony morphology (smaller plaque, edge smooth and round) and defected in biofilm formation in contrast with the wild-type (WT) strains. Further analyses indicated that the *aceE* gene deficiency affected the cell mycolic acid profile of *M. smegmatis*.

Methods

Strains, medium, condition

A transposon library was generated using *M. smegmatis* mc^2155 as previously described [1, 13]. The library was plated on 7H10 agar containing 20 mg/L kanamycin. Approximately 1000 single colonies of variable sizes were randomly picked into 96 deep well plates containing 0.5 mL of Middlebrook 7H9 medium (BD Difco) with kanamycin and grown at 37 ℃. After 5 days of growth, cultures from each well were spotted on the Middlebrook 7H10 agar (BD Difco) plates. *E. coli* strain DH5α *pir 116* (kindly provided by Dr. Kaixia Mi) was used to identify the insertion site of the transposon mutant. *E. coli* strain Top10 (TransGen Biotech, China) was used to clone specific DNA fragments into pSMT3 plasmid (Table 1). When required, kanamycin (50 mg/L for *E.coli* and 20 mg/L for mycobacteria) and hygromycin (150mg/L for *E.coli* and 75 mg/L for mycobacteria) were added to the growth medium.

Transposon identification

To identify mutants with growth defects, genomic DNA was prepared from the selected transposon mutant. The genomic DNA was randomly digested with *BamH*I (Fermentas International Inc.) and then purified with a DNA extraction kit (Fermentas International Inc.). The purified DNA was ligated and transformed into DH5α *pir116* competent cells. The plasmids from the kanamycin-selected positive colony were isolated and sequenced with following primers: TLP1 5’-GCTGACCGCTTCCTCGTGCTTTA-3’; TLP2 5’-GCAGCGCATCGCCTTCTATC-3’.

Construction of complemented strain of *aceE*-mut

For complementation of *aceE*-mut strain, 2.7 kb full-length *aceE* gene from *M. smegmatis* was cloned into the mycobacterial shuttle vector pSMT3[14] using NEBuilding pfu kit (New England Biolabs, Ipswich, MA), to generate pSMT3-*aceE* (Table 1). The plasmid pSMT3-*aceE* was subsequently transformed into *aceE*-mut strain to

generate the complemented strain i.e. Comp (Table 1). The transformants were selected on 7H10 agar plates, supplemented with 20 mg/L kanamycin and 75 mg/L hygromycin, followed by incubation at 37 ℃ for 3–4 days. The positively grown clones were picked and identified by PCR-sequencing methods using following primers:

aceE_S-FP1 CGGGCTGCAGGAATTCGATTTGACCACCGAGTTCG

aceE_S-RP1 GACGGTATCGATAAGCTTGATTCAGGCGCTGCCGGTG

Colony morphology observation

To compare the colony sizes for different mycobacterial strains, log phase cultures were 10× serially diluted (1:10), grown on 7H10 medium at 37 ℃ and examined visually for any change. Photographs were taken after 3–4 days of incubation using stereo microscope (Leica MZ APO).

Morphology of *aceE*-mut strains by electron microscopy

Mycobacteria from log phase were harvested and washed with 0.1M phosphate buffer (PBS). Cells were subsequently fixed using 2.5% glutaraldehyde. Post fixation was carried out in 1% osmic acid. Following several rinses with ddH_2O, samples were dehydrated in a series of different concentrations of ethanol and 100% acetone. For transition solvent, resin:acetone (2:1) were used overnight. Epoxy resin-812 was used for 1 h for embedding. 90 nm sections were cut and stained with uranyl acetate and Reynold's lead citrate (Ted Pella, Inc). After drying, transmission electron microscopic images of the sections were taken using TEM-1400plus. The cell wall thickness of each strain was measured as follows: 100 mycobacteria in the visual field were randomly selected, the largest distance between the outer membrane and the inner membrane of each cell was measured, and the data were statistically analyzed. For scanning electron microscopy, ethanol dehydrated samples were dried in freeze-drier and coated with 10 nm gold film using ion sputter. Scan electron microscopic images were taken using SEM-6000F.

Estimation of biofilm formation

Biofilm formation was measured in M63-based liquid medium as previously described [15, 16]. Biofilms of all

three strains were grown in 96-well polystyrene plates or glass tubes containing M63-based liquid medium complemented with casein hydrolysate and glucose (without Tween-80), inoculated with 0.1% log phase culture, and incubated at 30 ℃ for 5–7 days under static conditions. The biofilm formation in each of the liquid cultures was qualitatively analyzed by photography and quantified with crystal violet staining, as previously described [15, 16].

Growth profile of strains

The growth characteristics of *M. smegmatis* mc^2155, *aceE*-mut, Vector (*aceE*-mut:Vector) and Comp (*aceE*-mut:*aceE*) strains were studied in neutral 7H9 medium or acidified 7H9 medium (pH 5.0). The cultures were inoculated with an initial optical density at 600 nm (OD_{600}) of 0.01 and incubated at 37℃ with constant shaking at 200 rpm. OD_{600} were measured at a specified time intervals, and 10-fold serial dilutions were plated on 7H10 agar plates for CFU counts.

Stress assays

To carry out *in vitro* stress studies, logarithmic phase *M. smegmatis* cultures (OD_{600} ~ 0.8) were harvested and diluted cultures were subjected to different stresses. For oxidative stress, *M. smegmatis* cultures at OD_{600} (~0.4) were exposed to (hydrogen peroxide, 0.1% or 1%) and CFU was determined after 24 h. For other stresses, *M. smegmatis* cultures, prepared as above, were adjusted to OD_{600} = 0.4 and $NaNO_2$ or SDS was added. CFU was determined after 1 h with SDS and after 24 h with $NaNO_2$.

Antimicrobial susceptibility testing

Minimal Inhibitory Concentration (MIC) determination was performed by using the alarm blue microtiter assay as recommended in CLSI guidelines [9].

Mycolic acid analysis using HPLC-Sherlock mycobacterium identification system

The growing bacterial liquid was collected for isolation of mycolic acids in the cell walls by extraction, saponification, and derivation according to instructions for the Sherlock Mycobacteria Identification System (SMIS;

MIDI, Inc.). Mycolic acid composition of each sample was analyzed by SMIS using HPLC.

Analysis of the composition of mycolic acids and lipids using LC-MS

Analysis of mycolic acids and lipids were carried out using normal-phase LC-MS as previously described, with minor modification [17, 18]. The experiments were conducted with the help of Lipidall Technologies Company Limited (Changzhou, Jiangsu, China). Briefly, the Exion uplc-qtrap 6500 PLUS (Sciex) liquid-mass spectrometer was used for all of the experiments whereas the electric spray ionization (ESI) mode was used for all the analyses. The following conditions were used: curtain gas = 20, ion spray voltage =5500 V, temperature = 400 ℃, ion source gas 1 = 35, and ion source gas 2 = 35. Lipids were extracted from the samples using an improved Bligh/Dyer extraction method (twice extraction) and appropriate internal standards were added. Phenomenex Luna 3-micron silica column (inner diameter 150x2.0mm) was used to separate different kinds of polar lipids using mobile phase A (chloroform: methanol: ammonia 89.5:10:0.5) and B (chloroform: methanol: ammonia: water 55:39:0.5:5.5) using NP-HPLC. The gradient of mobile phase A was maintained for 5 min from 95%, then linearly decreased to 60% within 7 min and maintained for 4 min, and then it was further reduced to 30% and maintained for 15 min. Finally, the initial gradient was maintained for 5 min. Multiple reactions monitoring (MRM) conversion was established for the comparative analysis of various polar lipids and the signal intensity of each MRM value was normalized to an internal standard for quantitative comparisons

Macrophage infections

Infection of THP-1 cell was performed using the RPMI1640 pre-washed *mycobacteria* at a multiplicity of infection (MOI) of 10:1 and 1:1 (bacteria: macrophage). For mycobacterium intracellular study, infected macrophages were harvested at 24h and 48h, and lysed with 0.1%Tween-80. Then the lysates were serially diluted with 0.05%Tween-80, and plated on 7H10 agar plates with or without the antibiotic. The plates were incubated at 37 ℃

until colonies could be counted.

Statistical analysis

All statistical analyses were performed using SPSS statistics 21. The OD_{600} or CFU counts were analyzed using the one-way ANOVA (Kruskal–Wallis with Dunn's multiple test) when comparing more than two groups. For the biofilm formation quantification, Student's t test was used. For mycolic acid and lipid quantification experiments, Tukey's HSD test was used. Only *P* values < 0.05 were considered as statistically significant.

Results

The *aceE*-mut exhibited unusual colony morphology.

By screening the *M. smegmatis* transposon library, a transposon mutant showed obvious differences in colony morphology (small plaque, smooth without jagged edge, fruity and yellow color) on agar plate when compared to the parental WT *M. smegmatis* strain (Fig 1A). DNA sequencing and analysis of the MycoMar/*M. smegmatis* chromosomal junction revealed that the transposon mutant had an insertion at a TA dinucleotide within the *aceE* gene (Fig 1B and C). No apparent difference in growth rate was found between the WT and *aceE*-mut strain with the Middlebrook 7H9 neutral medium culturing (Fig 2A and B). However, we observed that the *aceE*-mut strain dispersed uniformly in the broth without Tween-80, while the WT *M. smegmatis* agglomerated easily in the same medium. Notably, the growth rate of *aceE*-mut was significantly slower than WT strain in the acidified 7H9 media during the logarithmic phase and the stationary phase (Fig 2C and D). Comp strain demonstrated similar growth dynamics as WT in both culture conditions. These results demonstrated that the disruption of *aceE* gene in *M. smegmatis* renders the bacteria more sensitive to acid stress, and this feature could be complemented with the wild-type copy of *aceE* gene.

Pellicle and biofilm formation defected in *aceE*-mut

In contrast to the significant pellicle growth that appeared on the air-liquid interface in the WT strain culture, pellicle was absent from the *aceE*-mut strain culture when grown in 7H9 medium without Tween-80 supplement and shaking (data not shown). In order to better quantify the defect of *aceE*-mut in biofilm formation, strains were cultivated in M63-based liquid medium. Consistently, *ace*E-mut did not form biofilm in the M63-based liquid medium either. Notably, the complementary expression of *aceE* gene in *aceE*-mut strain restored the pellicle and biofilm formation to the WT levels (Fig 3A and B). Taken together, these results indicated that *aceE* gene is involved in pellicle and biofilm formations.

aceE gene affected the cell surface morphology and cell wall architecture of _M. smegmatis_

The surface morphology of WT and *aceE*-mut was observed by scanning electron microscopy. The *aceE*-mut cells were slightly shorter than WT cells, and their surfaces were smoother than WT cells (Fig 4).These microscopic observations were consistent with the smooth phenotype on agar plate. The cell morphology and cell wall architecture were further examined by transmission electron microscopy, which observed that cell wall of the mutant was slightly thinner than WT cell (Fig 5).

Cell wall permeability analysis

In order to analyze the effect of disruption of the *aceE* gene on the cell response to stress conditions *in vitro*, the *aceE*-mut and WT strains were treated with 12 anti-TB drugs and several antimicrobial agents *in vitro*. In contrast with the WT strain, the sensitivity of *aceE*-mut to various antibiotics (including isoniazid, rifamipin, ethambutol, streptomycin, capreomycin, amikacin, ethionamide, p-aminosalicylic acid, ofloxacin, levofloxacin, rifabutin and clathromycin) remained unchanged (data not shown). However, the mutant strain was slightly more sensitive to $NaNO_2$, H_2O_2, and SDS (Supplementary Fig S1).

Disruption of _aceE_ gene affected the Mycolic acid composition

The mycolic acid (C_{60} ~C_{90}) composition was analyzed by HPLC using Mycobacteria Identification System. In contrast to WT strain, mutant strain possessed higher proportion of short-chain mycolic acids but lower proportion of long-chain mycolic acids (Supplementary Fig S2), suggesting a potential role of *aceE* gene in mycolic acid metabolism. A further LC-MS-based systematic analysis of mycolic acid and lipids did not identify any obvious differences in the phospholipid and glycolipid compositions between the WT and *aceE*-mut strains (data not shown), whereas some kinds of mycolic acids (e.g. alpha-MA and epoxy-MA) were deficient in *aceE*-mut strains and these changes were fully restored upon complementation (Fig. 6).

Discussion

Transposon mutagenesis has been used extensively as a useful tool for studying gene function of mycobacteria. In this study, using transposon mutagenesis method we found an *aceE* gene mutant presenting a deficient colony morphology on 7H10 agar. Hence, it is reasonable to speculate that this mutant may have defects in cell wall biosynthesis. Changes in the structure of cell envelope components may affect the normal physiological metabolic process of mycobacteria, such as the intake of nutrients, antimicrobial agents' transportation across the plasma membrane and mycobacterial survival in stress condition, etc.

Previous studies have shown that mycobacterial PDH genes (*aceE*, *dlaT* and *lpd*) are not only involved in pyruvate metabolism, but may also have more complex biological functions. In contrast with *Escherichia coli*, whose PDH genes are located in an operon, the PDH genes of mycobacterium are regulated by different operons [19]. At present, only the PDH genes of mycobacteria and its close relative, corynebacteria, have been found to transcript independently, suggesting additional functions of these genes. In mycobacteria, the transcription of *dlaT* gene is independent of other PDH genes (*aceE* and *lpd*). It has been observed that *dlaT* gene knockout significantly affects the i*n vitro* growth of TB bacilli in the standard medium. The mutant is not only sensitive to reactive nitrogen intermediates but its virulence is also reduced in infected mice. In addition, the study found that *dlaT* inhibitors can selectively kill non-self-replicating TB bacilli, suggesting that *dlaT* gene may associate with latent TB infection in host cells [20-22]. Study also showed that the disruption of *lpd* gene in Mtb leads to decreased virulence with lower bacterial load in lung and other organs in infected mice. Other study revealed that the LPD is a component of branched chain ketones acid dehydrogenase, which takes part in succinyl CoA metabolism of amino acids such as valine (Vla), isoleucine (Ile) [23].

In contrast, the E1 component of mycobacterial PDH is beyond well-understood. In 2005, Tian et al., confirmed for the first time that *aceE* gene is the coding gene of the E1 component of PDH complex in Mtb [24]. In 2008, Li's

study found that the expression level of *aceE* gene in H37Rv was significantly higher than that of H37Ra during the course of macrophages infection [25]. This result is consistent with the results of gene chip analysis conducted by Manganelli et al. in 2001 [26]. Earlier studies had shown that H37Rv respiration is stronger than H37Ra. Although both the virulent H37Rv and the non-virulent H37Ra strains, rely on glycolysis and aerobic respiration for glucose metabolism, it is believed that glucose metabolism in H37Rv may be more dependent on the glycolytic pathway [27, 28]. Therefore, it is speculated that the up-regulated expression of *aceE* gene enables it to not only participate in aerobic respiration as a component of PDH, but also guarantee successful glycolysis under the hypoxic conditions and thus provide excellent energy supply for the growth of the virulent strain H37Rv. Another study showed that AceE component of PDH forms a four-component peroxidase system with DlaT/AhpD/AhpC that is involved in reductase reaction using pyruvate as electronic supply. Besides, it revealed that tuberculosis bacillus may recruit some intermediate metabolites to activate the defense system against the host's active nitrogen and evade host immune surveillance. All of the above studies have suggested that *aceE* gene plays an important role in Mtb metabolism *in vitro* and *in vivo.*

In the present study, we screened the random transposon mutants and found that the inactivation of *aceE* gene affects the colony morphology and biofilm formation in *M. smegmatis* which suggests its potential to affect the lipid metabolism and cell wall. The findings obtained in our study are in agreement with those of Viswanathan. et al.[29], but they only described such phenomenon without delving into its mechanism. Integrity of the cell wall has important biological significance on the *in vitro* and *in vivo* survival for bacteria. To further investigate the characteristics of the *aceE*-mut, series of assays were performed to compare the phenotypes of *aceE*-mut with the WT strains. We further analyzed the key composition of mycolic acid of each strain and identified altered composition of mycolic acid in *aceE*-mut which suggests that this gene may involve in the metabolism of mycolic acid in mycobacteria. Therefore, it was necessary to thoroughly analyze the cell wall composition of both WT and

aceE-mut strains and explores the role of *aceE* gene in the process of cell wall synthesis and metabolism. Comparative analysis of the lipid and mycolic acid profiles of the *M. smegmatis aceE*-mut, *M. smegmatis* WT and the Comp using LC-MS indicated that the metabolism of some kinds of alpha-MA and epoxy-MA was deficient in *aceE*-mut, which demonstrated its role in mycobacterial mycolic acid metabolism. In addition, we observed that the *aceE*-mut have a distinct cell morphology and ultrastructural appearance compared to WT strain when grown in broth culture that may result from the inability of the mutant to synthesize certain kinds of mycolic acids. The inactivation of *aceE* also impacts bacterial physiology that range from reduced biofilm formation to changes in the cell size and cell wall thickness. Most importantly, *aceE*-mut was more susceptible to acidic stress environments than the parental *M. smegmatis*, suggesting plausible role of *aceE* gene in stress tolerance inside the host.

aceE gene is more readily expressed in the virulent Mtb H37Rv (than H37Ra) throughout the course of infection, that not only suggests its important role in the virulence, survival and persistence of Mtb, but also makes this gene a potential target for the development of new TB vaccines and anti-TB drugs. Using blast tools, *aceE* gene sequence of *M. smegmatis* was analyzed which highlighted its conservation in *M. smegmatis* and a similarity of 82% with the *aceE* gene in Mtb. As a model bacterium widely used in the study of functional genes of mycobacterium, *M. smegmatis* can also be used to investigate the potential role of *aceE* gene in mycobacterial cell wall biosynthesis. In the present study, the stress assay demonstrated that *aceE* gene helped mycobacteria to withstand acidic stress environment that also suggests its plausible role in stress tolerance inside host. However, macrophage infection study showed that the inactivation of *aceE* gene in *M. smegmatis* does not affect the bacteria proliferation in macrophages (data not shown). Since *M. smegmatis* does not have pathogenicity, the study using this bacterium model cannot reveal the possible function of *aceE* gene in Mtb pathogenesis. Therefore, the role of *aceE* gene in pathogenesis requires to be further explored using the virulent Mtb H37Rv strain.

Conclusions

An *aceE* mutant *M. smegmatis* mc^2155 strain selected from transposon library presented small, fruity morphology without jagged edge. Compared with its parental WT strain, *aceE*-mut lost the ability of growing aggregately and biofilm formation, and became more fragile to acidic stress. Additionally, alteration of the mycolic acid profile in *aceE*-mut may directly impact the overall cell wall morphology and acid sensitivity. All these changes of the mutant strain demonstrate that *aceE* plays an important role in mycobacteria.

Declarations

Abbreviations

PDH: pyruvate dehydrogenase complex; aceE-mut: aceE-deficient mutants; WT: wild-type; MA: mycolic acid; Mtb: *Mycobacterium tuberculosis*; anti-TB: anti-tuberculosis; MIC: Minimal Inhibitory Concentration; SMIS: Sherlock Mycobacteria Identification System; ESI: electric spray ionization; MRM: Multiple reactions monitoring;

Ethics approval and consent to participate: Not applicable

Consent for publication: Not applicable

Availability of data and material: The datasets used and analyzed during the current study are available from the corresponding author.

Competing interests: The authors declare that they have no competing interests.

Funding: The work was supported by National Natural Science Foundation of China (No. 31600107 and No. 81672065), Beijing Natural Science Foundation (No.5192006), National Major Science and Technology Projects of China (2018ZX10302-301-004), Tong Zhou "Yun He" Talent Project (YHLD2018030), Beijing Municipal Administration of Hospitals' Ascent Plan (DFL20181602), and Beijing Municipal Administration of Hospitals Clinical Medicine Development of Special Funding Support (ZYLX201809).

Authors' contributions: CST and HHR conceived and designed the experiments. CST, TTL, WSA, and ZTT performed the experiments. CST analyzed the data and was the major contributor in writing the manuscript. All authors have read and approved the manuscript.

Acknowledgements: We thank Prof. Guanghou Shui for his kindly help in lipid data reanalysis and helpful discussions.

Reference

1. Sassetti CM, Boyd DH, Rubin EJ. Comprehensive identification of conditionally essential genes in mycobacteria. P Natl Acad Sci USA. 2001;98(22):12712-7; doi: 10.1073/pnas.231275498.
2. Singhania A, Wilkinson RJ, Rodrigue M, Haldar P, O'Garra A. The value of transcriptomics in advancing knowledge of the immune response and diagnosis in tuberculosis. Nat Immunol. 2018;19(11):1159-68; doi: 10.1038/s41590-018-0225-9.
3. Russell DG. Mycobacterium tuberculosis: here today, and here tomorrow. Nat Rev Mol Cell Biol. 2001;2(8):569-77; doi: 10.1038/35085034.
4. Barry CE, 3rd, Boshoff HI, Dartois V, Dick T, Ehrt S, Flynn J, et al. The spectrum of latent tuberculosis: rethinking the biology and intervention strategies. Nat Rev Microbiol. 2009;7(12):845-55; doi: 10.1038/nrmicro2236.
5. Goodsmith N, Guo XV, Vandal OH, Vaubourgeix J, Wang R, Botella H, et al. Disruption of an M. tuberculosis Membrane Protein Causes a Magnesium-dependent Cell Division Defect and Failure to Persist in Mice. PLoS Pathog. 2015;11(2):e1004645; doi: 10.1371/journal.ppat.1004645.
6. Pandey AK, Sassetti CM. Mycobacterial persistence requires the utilization of host cholesterol. Proc Natl Acad Sci U S A. 2008;105(11):4376-80; doi: 10.1073/pnas.0711159105.
7. Chatterjee D. The mycobacterial cell wall: structure, biosynthesis and sites of drug action. Curr Opin Chem Biol. 1997;1(4):579-88; doi: S1367-5931(97)80055-5.
8. Daffe M, Draper P. The envelope layers of mycobacteria with reference to their pathogenicity. Adv Microb Physiol. 1998;39:131-203.
9. Clinical and Laboratory Standards Institute. Susceptiblity Testing of Mycobacteria, Nocardiae, and other Aerobic Actinomycetes; Approved Standard-Second Edition. Clinical and Laboratory Standards Institute. 2011.
10. Martin E, Rosenthal RE, Fiskum G. Pyruvate dehydrogenase complex: metabolic link to ischemic brain injury and target of oxidative stress. J Neurosci Res. 2005;79(1-2):240-7; doi: 10.1002/jnr.20293.
11. Schnappinger D, Ehrt S, Voskuil MI, Liu Y, Mangan JA, Monahan IM, et al. Transcriptional Adaptation of Mycobacterium tuberculosis within Macrophages: Insights into the Phagosomal Environment. J Exp Med. 2003;198(5):693-704; doi: 10.1084/jem.20030846.
12. Timm J, Post FA, Bekker LG, Walther GB, Wainwright HC, Manganelli R, et al. Differential expression of iron-, carbon-, and oxygen-responsive mycobacterial genes in the lungs of chronically infected mice and tuberculosis patients. Proc Natl Acad Sci U S A. 2003;100(24):14321-6; doi: 10.1073/pnas.2436197100.
13. Bardarov SS, Bardarov SS, Jr., Jacobs WR, Jr. Transposon mutagenesis in mycobacteria using conditionally replicating mycobacteriophages. Methods in molecular medicine. 2001;54:43-57; doi: 10.1385/1-59259-147-7:043.
14. Golanska E, Brzostek A, Kiatpapan P, Dziadek J. Characterisation of a new host-vector system for fast-growing mycobacteria. Acta Microbiol Pol. 1998;47(4):335-43.
15. Recht J, Kolter R. Glycopeptidolipid acetylation affects sliding motility and biofilm formation in Mycobacterium smegmatis. Journal of Bacteriology. 2001;183(19):5718-24; doi: Doi 10.1128/Jb.183.19.5718-5724.2001.
16. Recht J, Martinez A, Torello S, Kolter R. Genetic analysis of sliding motility in Mycobacterium smegmatis. Journal of Bacteriology. 2000;182(15):4348-51; doi: Doi 10.1128/Jb.182.15.4348-4351.2000.
17. Lam SM, Tong L, Duan XR, Petznick A, Wenk MR, Shui GH. Extensive characterization of human tear fluid collected using different techniques unravels the presence of novel lipid amphiphiles. J Lipid Res. 2014;55(2):289-98; doi: 10.1194/jlr.M044826.

18. Gong H, Li J, Xu A, Tang Y, Ji W, Gao R, et al. An electron transfer path connects subunits of a mycobacterial respiratory supercomplex. Science. 2018;362(6418); doi: 10.1126/science.aat8923.
19. Stephens PE, Darlison MG, Lewis HM, Guest JR. The pyruvate dehydrogenase complex of Escherichia coli K12. Nucleotide sequence encoding the dihydrolipoamide acetyltransferase component. Eur J Biochem. 1983;133(3):481-9.
20. Cole ST, Brosch R, Parkhill J, Garnier T, Churcher C, Harris D, et al. Deciphering the biology of Mycobacterium tuberculosis from the complete genome sequence. Nature. 1998;393(6685):537-44; doi: 10.1038/31159.
21. Shi S, Ehrt S. Dihydrolipoamide acyltransferase is critical for Mycobacterium tuberculosis pathogenesis. Infect Immun. 2006;74(1):56-63; doi: 10.1128/IAI.74.1.56-63.2006.
22. Bryk R, Gold B, Venugopal A, Singh J, Samy R, Pupek K, et al. Selective killing of nonreplicating mycobacteria. Cell Host Microbe. 2008;3(3):137-45; doi: 10.1016/j.chom.2008.02.003.
23. Venugopal A, Bryk R, Shi S, Rhee K, Rath P, Schnappinger D, et al. Virulence of Mycobacterium tuberculosis depends on lipoamide dehydrogenase, a member of three multienzyme complexes. Cell Host Microbe. 2011;9(1):21-31; doi: 10.1016/j.chom.2010.12.004.
24. Tian J, Bryk R, Shi S, Erdjument-Bromage H, Tempst P, Nathan C. Mycobacterium tuberculosis appears to lack alpha-ketoglutarate dehydrogenase and encodes pyruvate dehydrogenase in widely separated genes. Mol Microbiol. 2005;57(3):859-68; doi: 10.1111/j.1365-2958.2005.04741.x.
25. Li AH, Lam WL, Stokes RW. Characterization of genes differentially expressed within macrophages by virulent and attenuated Mycobacterium tuberculosis identifies candidate genes involved in intracellular growth. Microbiology. 2008;154(Pt 8):2291-303; doi: 10.1099/mic.0.2008/019661-0.
26. Manganelli R, Voskuil MI, Schoolnik GK, Smith I. The Mycobacterium tuberculosis ECF sigma factor sigmaE: role in global gene expression and survival in macrophages. Mol Microbiol. 2001;41(2):423-37; doi: 10.1046/j.1365-2958.2001.02525.x.
27. Heplar JQ, Clifton CE, Raffel S, Futrelle CM. Virulence of the tubercle bacillus. I. Effect of oxygen tension upon respiration of virulent and avirulent bacilli. J Infect Dis. 1954;94(1):90-8.
28. Murthy PS, Sirsi M, Ramakrishnan T. Tricarboxylic acid cycle and related enzymes in cell-free extracts of Mycobacterium tuberculosis H37Rv. Biochem J. 1962;84:263-9.
29. Viswanathan G, Joshi SV, Sridhar A, Dutta S, Raghunand TR. Identifying novel mycobacterial stress associated genes using a random mutagenesis screen in Mycobacterium smegmatis. Gene. 2015;574(1):20-7; doi: 10.1016/j.gene.2015.07.063.

Table 1. Strains and plasmids used in this study

Strain or plasmid	Relevant characteristic	Source or reference
Strains		
M. smegmatis mc^{2}155	WT	ATCC
aceE-mut	mc^{2}155 with *aceE*-mut disrupted by Himar1 transposon	This study
Vector	*aceE*-mut complemented with pSMT3-M plasmid	This study
Comp	*aceE*-mut complemented with pSMT3-*aceE*	This study
Plasmids		
Mar T7		(Bardarov et al., 2001
pSMT3	Carries *hyg*^{r}, *E. coli*-mycobacterial shuttle vector	Golanska et al., 1998
pSMT3-*aceE*	*aceE* gene cloned under *hsp60* promoter in pSMT3-M vector	This study

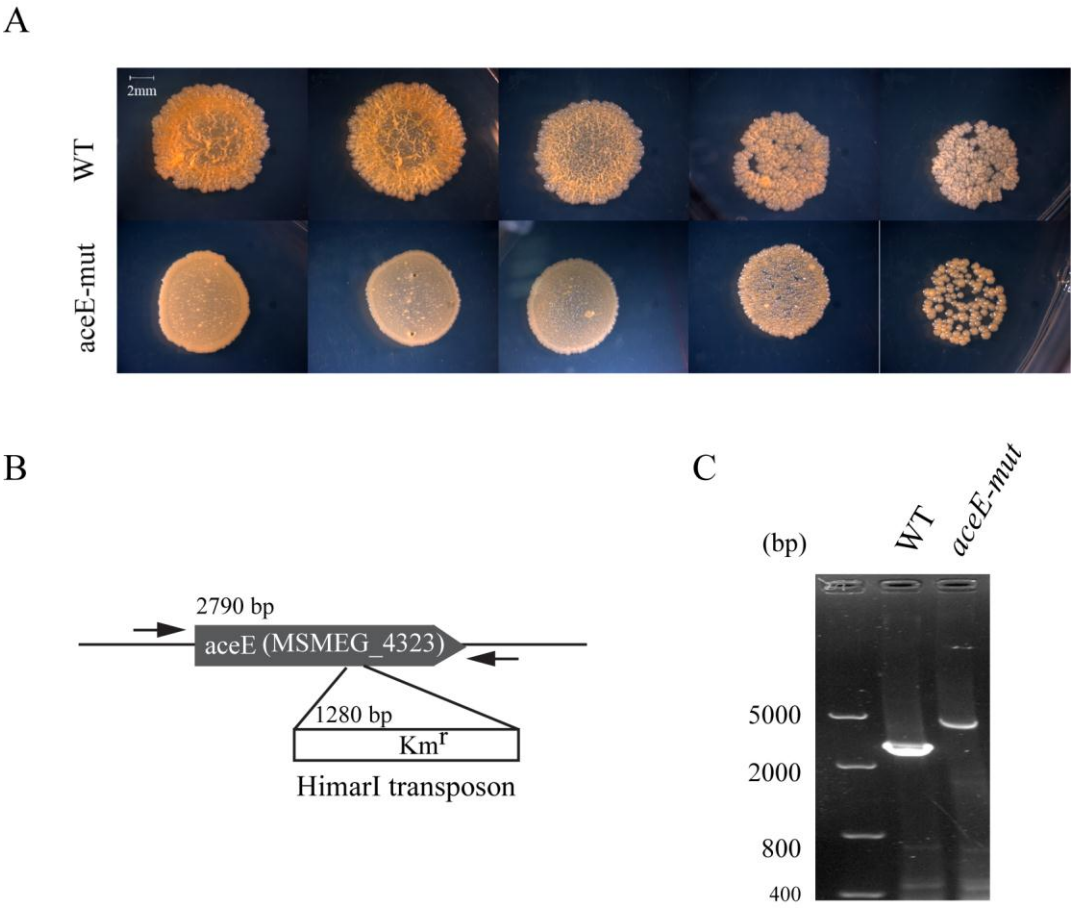

Figure 1. The identification of *M. smegmatis aceE*-mut. A. The *aceE*-mut showed smoother colony morphology in contrast to WT. The suspension of *M. smegmatis* mc^2155 and *aceE*-mut were spotted on the Middlebrook 7H10 medium supplemented with 0.2% glycerol. The images were taken after incubation at 37 ℃for 3 days on 7H10 plates. B. HimarI transposon insertion site in *aceE* gene; C. PCR verification of the *aceE* transposon mutant. WT: *M. smegmatis* mc^2155; *aceE*-mut: *aceE* gene deficiency mutant selected from *M. smegmatis* mc^2155 transposon library.

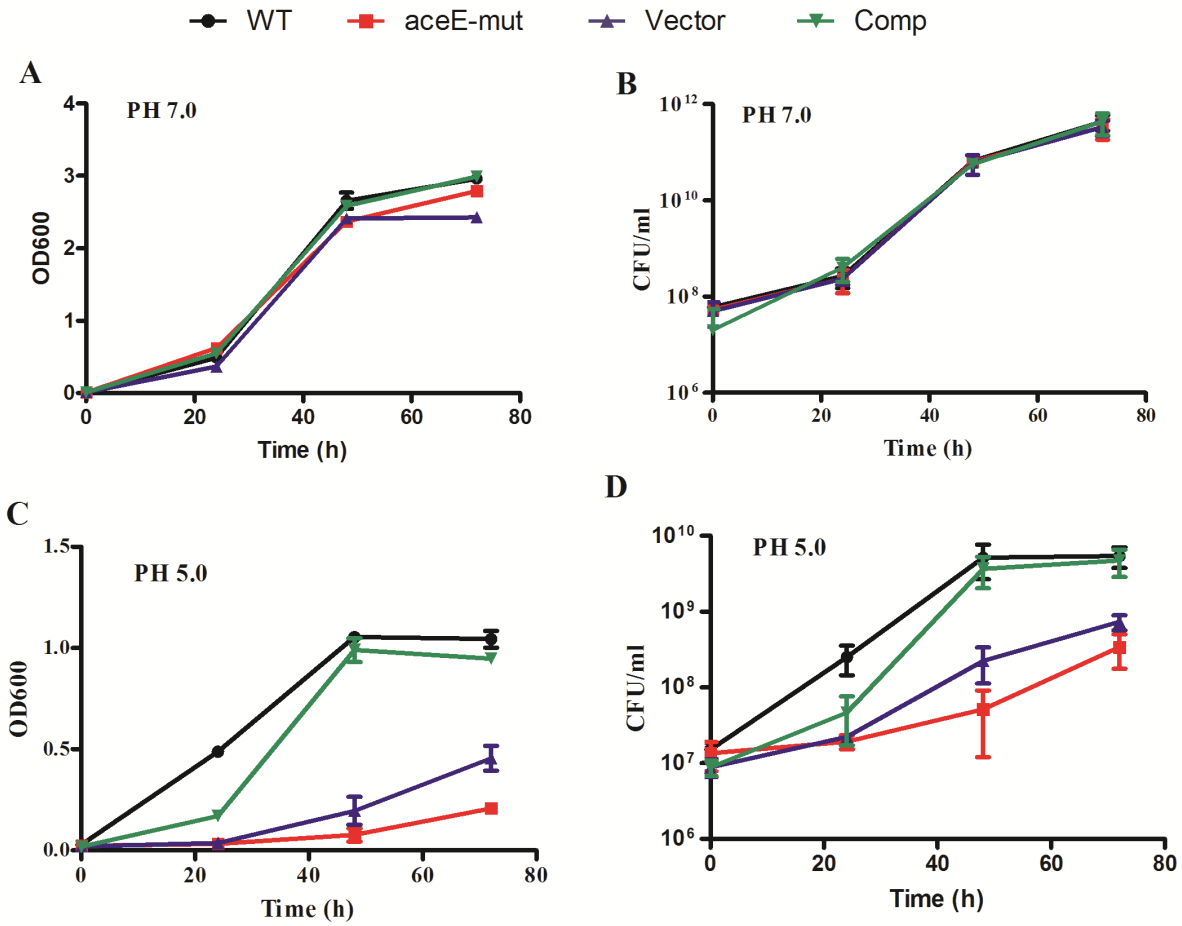

Figure 2. The *aceE*-mut strain was sensitive to acid stress. A and B. Bacterial strains were grown in the neutral Middlebrook 7H9 medium supplemented with 0.05% Tween-80 and 0.2% glycerol; C and D. Bacterial strains were grown in the acified Middlebrook 7H9 medium (PH5.0) supplemented with 0.05% Tween-80 and 0.2% glycerol. The OD_{600} and CFU were determined at an interval of 24 h. The graph is a representation of one of three independent experiments.

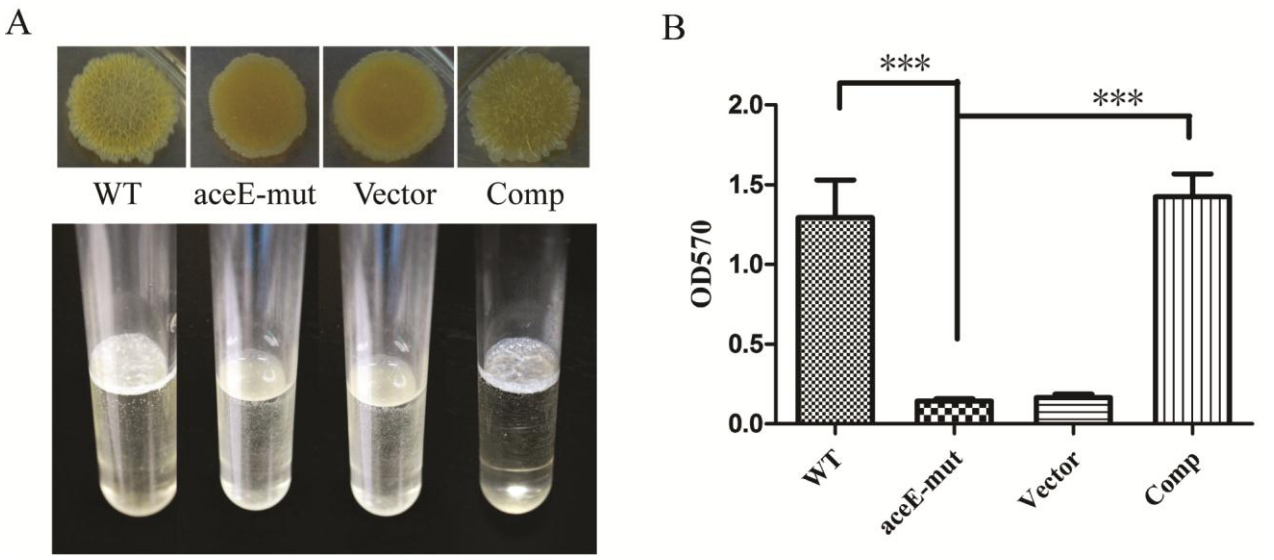

Figure 3. The effect of *aceE* deficiency on formation of mycobacterial biofilm in M63 medium. A. *aceE*-mut is defective in biofilm formation, while the complementary expression of *aceE* gene in *aceE*-mut stain can recover the formation of mycobacterial biofilm. Each experiment performed in triplicate. B. Quantification of the biofilm formation after crystal violet staining. Mean optical density for five biological replicates per strain ± SD for a representative experiment from 3 experiments is shown. Significant differences were determined by Student's t-test and are indicated by *** (P<0.001). Error bars represent SD.

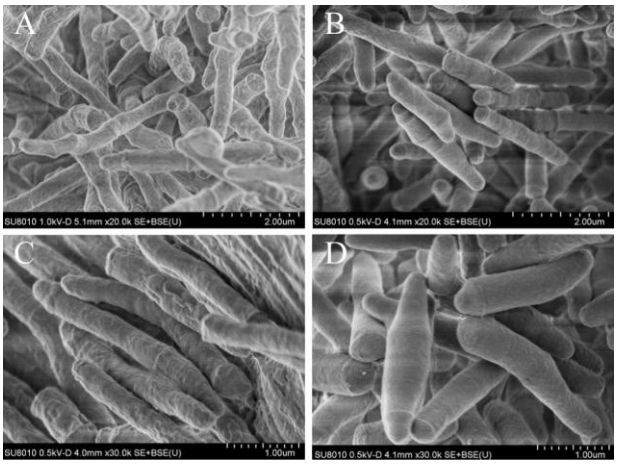

Figure 4. The morphology of *M. smegmatis* mc^2155 (A and C) and *aceE*-mut (B and D) under SEM. Bars represent 2 μm (A and B) and 1μm (C and D).

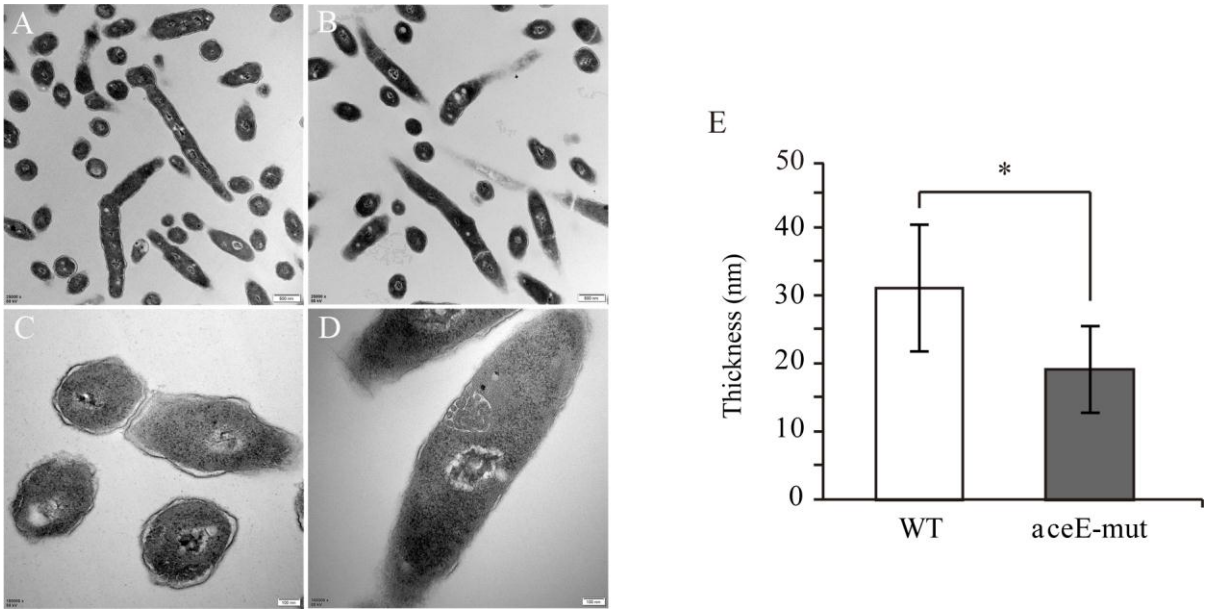

Figure 5. The cell wall thickness of *M. smegmatis* mc^2155 (A and C) and *aceE*-mut (B and D). E. The quantification of the cell wall thickness for WT and *aceE*-mut strains, one hundred mycobacteria in the visual field were randomly selected. The largest distance between the outer membrane and the inner membrane of each cell was measured and statistically analyzed. Bars represent 500nm (A and B) and 100nm (C and D). Histogram bars in panel E indicate standard deviation. Significant differences were determined by Student's t-test and are indicated by * (P<0.05).

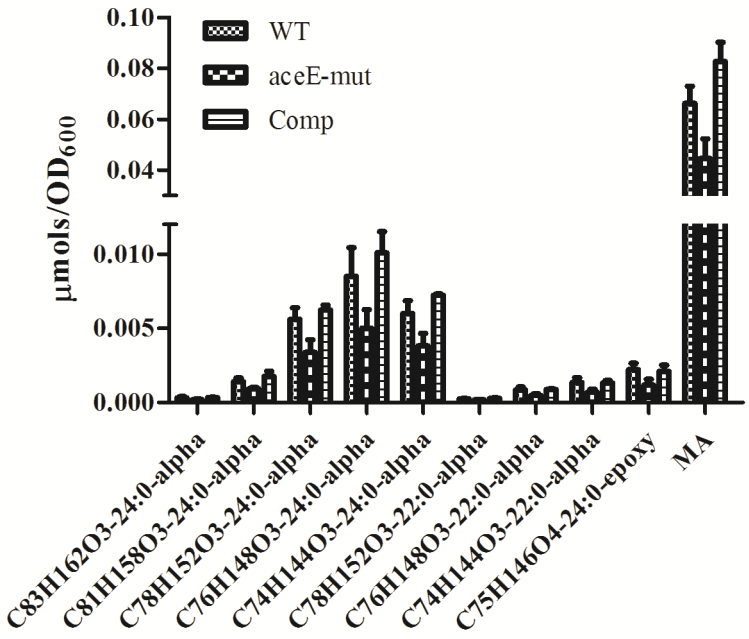

Figure 6. The effect of *aceE* deficiency on mycolic acid composition of mycobacterium. Only the components with significant difference in expression between aceE-mut and WT [and complementary (Comp)] strains were shown in the diagram (Tukey's HSD test). The bar depicts mean (±SD) for each group (n=4).

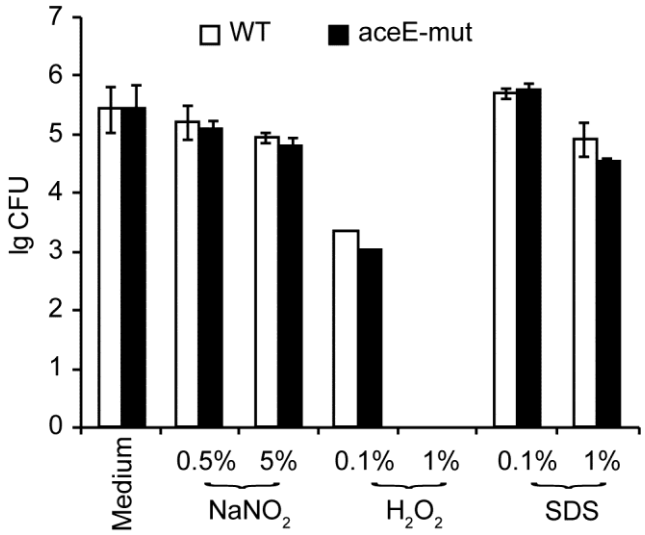

Supplementary Fig 1. Different growth of *M. smegmatis* mc^2155 (WT) and *aceE*-mut after treatment with different chemical agents.

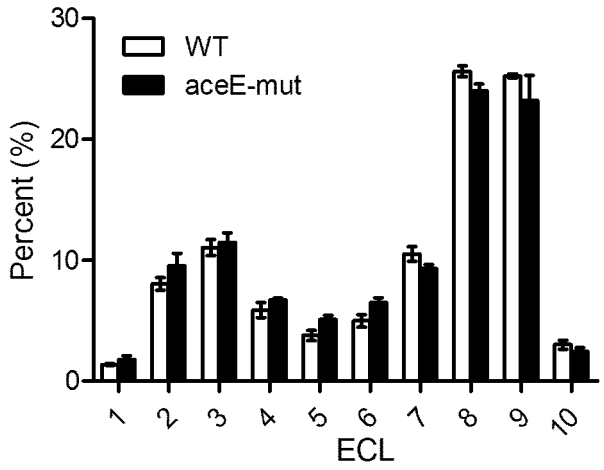

Supplementary Fig 2. The effect of *aceE* deficiency on mycolic acid composition of mycobacterium. ECL: the Equivalent Carbon Length of the mycolic acid.